A FRESH LOOK AT PREDICTIVE EQUATIONS FOR COMPRESSIONAL WAVE VELOCITY - POROSITY

N. Robin Brereton and David M. McCann
British Geological Survey, Keyworth, UK

Abstract The Wyllie time average equation has, for many years, been universally applied to predict porosities from compressional wave velocities, or visa-versa. However, it has long been recognized that the Wyllie equation does not adequately describe the actual relationship between these two parameters, and there have been many attempts to improve upon it. These have included the use of a simplified Wood equation, the concept of acoustic formation factor, and a wide range of empirical relationships. In many cases these models have been derived by testing them against a set of data representing a relatively narrow range of porosity values and, similarly, the use of the Wyllie equation has often been justified by virtue of a pseudo-linear relationship over a narrow range of porosity values.

Some of the limitations of the time average equation were also recognised by Wyllie and his co-workers who amended the Wood emulsion equation to partially take account of the rigidity of the materials. Further modifications to this Wyllie-Wood equation have been shown here to not only describe the relationship between porosity and velocity more closely than the time average equation, but also more closely than some of the alternative proposals suggested by contemporaries of Wyllie and since.

A semi-empirical acoustic impedance relationship has been developed which is shown to provide a more accurate porosity-velocity transform, using realistic material parameters, than has hitherto been possible.

INTRODUCTION

Between August 31 and November 1 1988 Leg 123 of the Ocean Drilling Program (ODP) investigated two sites in the deep Indian Ocean northwest of the Australian continental margin. The first of these (Site 765), is at the southern limit of the Argo Abyssal Plain within 50 Km of the Exmouth Plateau and the second (Site 766), about 850 Km to the southwest (Figure 1), is at the boundary between the ocean crust of the Cuvier and Gascoyne abyssal plains and the continental crust of the Exmouth Plateau.

One of the primary objectives of ODP Leg 123 was to drill the oldest sediments and basement of the Indian Ocean in the Argo Abyssal Plain to understand the paleoceanography, sedimentology, and magmatic processes relating to rifting of the northwestern Australian margin, the initiation of the Indian Ocean and the consequent destruction of the Tethyan seas. An important secondary objective was to create a geochemical reference site for ocean crust composition close to a subduction zone.

At Site 765 calcareous turbidites constituted more than 75% of the section, alternating with hemipelagic claystones, but the most surprising stratigraphic finding was the lack of any Jurassic sediments. Initial results indicate that the Indian Ocean opening started about 20 Ma later than had previously been thought (Berriasian-Valanginian as opposed to Oxfordian), requiring a significant revision of the plate-tectonic reconstruction of the northeastern Indian Ocean. The hole is in 5714 m of water and penetrated over 930 m of Cretaceous through Cenozoic sediments and a further 271 m of oceanic basement with relatively fresh, glass-bearing pillow lava and massive basalt. It was necessary to case-out the sediments before drilling the basement and this involved installing a re-entry cone. The drillship "JOIDES Resolution" achieved the deepest steel cased-hole in the worlds oceans and the hole has been left in excellent condition for further drilling on future legs.

Site 766, in 4 Km of water penetrated 220 m of locally derived terrigenous clastic fan deposits overlain by 240 m of pelagic ooze, chalk and chert. The basal sediments are intruded by basalt sills and a massive dyke, almost continuously recovered for about 60 m.

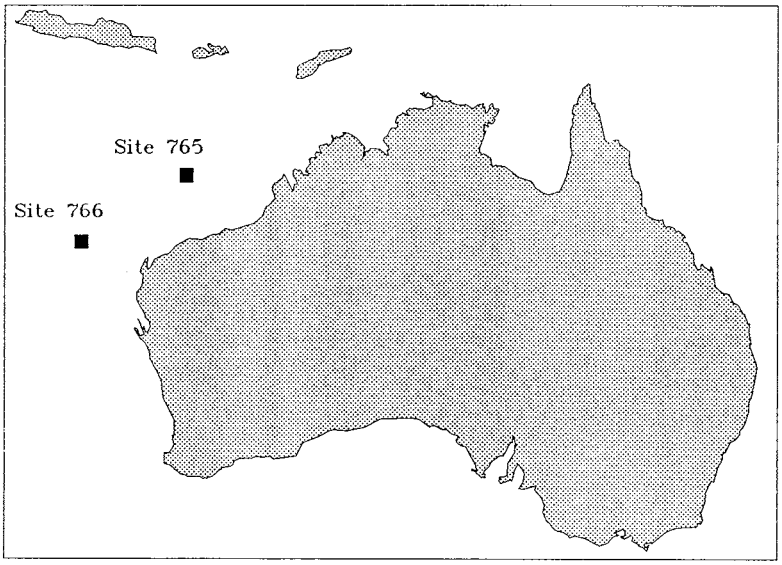

FIGURE 1 ODP Leg 123 drilling site locations.

Preliminary results from the wide ranging scientific investigations carried out during the Leg 123 cruise are in preparation or have been briefly reported (ODP Leg 123 shipboard scientific party. 1989a, 1989b and 1990) but the principal findings are to be published in the Proceedings of the Ocean Drilling Program - Scientific Results (Vol 123).

PHYSICAL PROPERTY MEASUREMENTS

Physical properties determined on board ship were: porosity, bulk density, grain density and water content (collectively referred to as index properties); and compressional wave velocity.

Drilling technology employed by the ODP enables continuous coring of the softest sediments at the seawater-sediment boundary, right through to the hardest basalts. The cores were recovered in 10 m plastic sleeved core barrels thereby retaining the integrity of the softer materials. Soon after core recovery, the plastic liners were cut into 1.5 m

sections and each section split lengthwise. One half was archived while the other was used for sampling. Samples for index property and compressional wave velocity measurements were taken by either cutting parallel sided pieces with a knife in the softer sediments, or using a double bladed diamond saw for the more brittle or lithified sediments. Basement rock samples were obtained using a 2.5 cm rock corer. In almost all cases these two sets of measurements were made on the same samples. At no time were the cores allowed to dry out prior to measurements being taken and sample temperatures were allowed to equilibrate with the stabilised laboratory temperature.

For the index property determinations samples were weighed wet using two Scientech 202 electronic balances, interfaced with a micro computer, which compensates for the ship's motion by taking the average of 100 sample weighings. The wet sample volumes were determined by using a Quantachrome helium Penta-Pycnometer. Dry sample weights and volumes were determined using the same procedure after freeze drying the sample for 12 hours. The accuracy of the weight and volume determinations were periodically checked using calibration standards.

Compressional wave velocities were calculated from the determination of the travel time of a 500 kHz compressional wave through a measured thickness of sample using a Hamilton Frame Velocimeter and Tektronix DC 5010 counter/timer system. Travel distance was measured using an attached variable resistor connected to a Tektronix DM 5010 digital multimeter. It was found that a calibration correction factor of 1.0347 was needed to bring all the measured values into agreement with expected values. Sea water velocity determined on this basis was about 1560 m/s.

The index property and compressional wave velocity data were entered into the shipboard Physical Properties Data Collection System which computes the depth below sea floor (mbsf), index properties and velocity for each sample. All these data have been tabulated by Brereton (1990).

GEOLOGICAL SUMMARIES

Site 765

The sediments at Site 765 can be identified in terms of four basic physical properties units, namely, A (0-80 mbsf), B (80-350 mbsf), C (350-590 mbsf), and D (590-896 mbsf). No samples were taken from the intervals 646-675 mbsf and 896-936 mbsf as these represented sensitive stratigraphic boundaries.

Unit A consists of calcareous ooze with significant changes in the index properties. Unit B consists of debris flows and turbidites. In the interval from 265-290 mbsf the general lithology consists of homogeneous clay deposits sandwiched between thinner layers of carbonate cemented sands. Unit C consists of debris flows and turbidites with the sediments showing a much higher degree of lithification. The material alternates between claystone, chalk, and cemented sandstone with periodic intrusions of coarse sands and basalt pebbles. Unit D consists predominantly of a dark red claystone. The claystone is not as competent as the claystones in unit C and tended to slake or delaminate when exposed to water or became air dried. During sampling, the material had a "spongy" appearance. The boundary is readily distinguishable in terms of physical property changes.

The compressional wave velocity data showed an underlying trend of progressively increasing velocities, from approximately 1525 m/s in the calcareous ooze near the sea bottom sediment boundary, to about 2010 m/s near the sediment basement boundary. Superimposed on this trend are a series of high and low velocity excursions. The higher values are associated with lithified claystone, chalk or cemented sandstone, whereas low values are indicative of less lithified claystone, carbonates or poorly cemented sandstone. The variability in the data is also, in part, a result of the sampling procedure followed. Samples were taken to be as representative as possible of the sediment section as a whole. In the case of a turbidite or debris flow sequence, both the upper fine grained and lower coarse grained sequences were selected. Sample selection also depended upon the relative frequency, thickness, and homogeneity of a particular sequence; thin, unrepresentative lithologies were avoided. Basalt pebbles occurred relatively frequently in the

debris flow sequences, and were sampled at 465.56, 635.33 and 763.34 mbsf. These data represent significant spikes in the trends.

A series of high velocity peaks were observed between 350-450 mbsf. These peaks appear to be superimposed on a slight velocity increase between 350-590 mbsf and closely correspond to intermediate depth high amplitude reflectors recorded on the seismic survey lines (ODP Leg 123 Initial Reports volume). In addition, this section corresponds to the increased lithification of the sediments composing the turbidite and debris flow sequences. There is also a sharp decrease in velocity between 585.19 and 593.04 mbsf which also corresponds to a low amplitude reflector on the seismic profile.

The basement rocks were relatively homogeneous and composed primarily of pillow basalts and massive basalt flows. A sharp increase in water content and porosity occurred at 994 and 1005 mbsf with corresponding reductions in the measured velocity. These samples appeared lighter in colour and had a much coarser grain structure when compared with the other basalts. A reduction in velocity for the sample from 1140 mbsf corresponds to an interval in which a number of calcite veins were observed.

Site 766

The sediments at Site 766 can be identified in terms of five basic physical properties units, namely, A (0-100 mbsf), B (100-185 mbsf), C (185-240 mbsf), D (240-300 mbsf), and E (300-459 mbsf).

Unit A consists of calcareous ooze with significant changes in the index properties in the upper 22 mbsf, followed by more gradual changes which are consistent with normal compaction trends. Unit B consists of mixed sediment of claystone and chalk. Unit C consists predominantly of chalk with hard chert layers. Unit D consists predominantly of a dark brown to reddish brown claystone which tended to slake or delaminate when exposed to water or became air dried. Unit E is composed primarily of green to gray glauconitic siltstones and sandstones with periodic layers of highly lithified bioclastic sandstone. The lowermost 20 m consists of a gray to black clayey sandstone, although the index properties for this layer did not vary significantly from those described for the unit as a whole.

The compressional wave velocity progressively

increases to about 1900 m/s near the sediment-basement boundary. Superimposed on this trend were a series of high velocity excursions associated with the layers of chert and lithified bioclastic sandstone. A low velocity sample from 141 mbsf also corresponded to marked changes in the index properties and came from a less well lithified chalk section of a mixed sediment claystone-chalk sequence. Two velocity spikes at 201 and 222 mbsf corresponded to chert. At 300 mbsf and in the interval from 350 to 440 mbsf another series of velocity peaks correlated with highly lithified bioclastic sandstone layers.

The igneous rocks drilled at Site 766 consist of three basic units, namely, A (460-463 mbsf), B (463-467 mbsf), and C (467-516 mbsf).

Unit A is a thin basalt sill. The index properties varied considerably from the outside edges toward the centre. Unit B comprises a thin dark shale sediment layer, which was very similar to that observed in the lowermost portion of the sediment column and unit C consists of a thick diabase sill. Velocities for the uppermost basalt unit vary considerably from about 4200 m/s, at the upper and lower boundaries, to 5179 m/s at the centre. Within the sediment layer the velocity decreases significantly to an average value of 1848 m/s while the lowermost basalt unit shows some slight variations in the velocities, with an average of 5450 m/s.

INDEX PROPERTY CORRELATIONS

The index properties were determined from four measurements (wet volume, dry volume, wet weight, and dry weight) and according to the following definitions :

Porosity ϕ = volume of water / volume of wet core;
Bulk Density ρ_s = weight of wet core / volume of wet core;
Grain Density ρ_g = weight of dry core / volume of dry core;

From these definitions the following relationship can be derived:

$$\rho_s = \phi(\rho_p - \rho_g) + \rho_g \qquad (1)$$

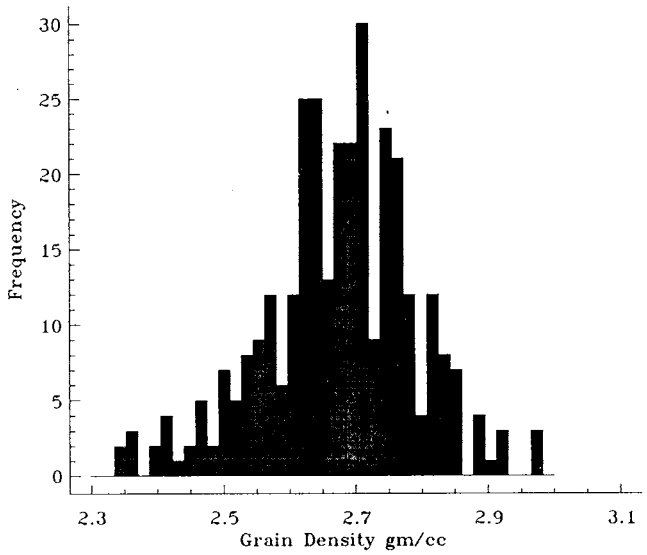

FIGURE 2 Histogram of sediment grain densities.

The algorithms used in the shipboard Physical Properties Data Collection System to calculate the index properties were corrected for salt content by assuming a pore water salinity of 36.3 ppt and a pore water density (ρ_p) of 1.0245 g/cm³.

A frequency histogram of grain densities for all the sediment samples from Sites 765 and 766 is shown in Figure 2. The data ranges from 2.16 to 3.22 g/cm³ but the average is 2.677 ± 0.134 g/cm³ with a geometric mean of 2.674 and a mode of 2.64. The cyclicity of the histogram suggests data groupings about grain density values of about 2.55, 2.64 (quartz), 2.71 (calcite), 2.75 and 2.82 g/cm³ with the majority falling in the quartz-calcite range. Similarly, the data range of grain densities for all the basalt samples lies between 2.66 and 2.97 g/cm³ with an average of 2.872 ± 0.064 g/cm³, a geometric mean of 2.871 and a mode of 2.85.

It follows from equation 1 that a plot of ρ_s against ϕ, will yield an intercept of ρ_g and a slope of $(\rho_p - \rho_g)$. Such a plot for all the sediment samples and all the

basalt samples is shown in Figure 3. A linear regression through the sediments gives an equivalent grain density of 2.667 ± 0.017 g/cm³, a pore fluid density of 1.034 g/cm³ (slope = -1.633 ± 0.032), with an R^2 of 88.9%.

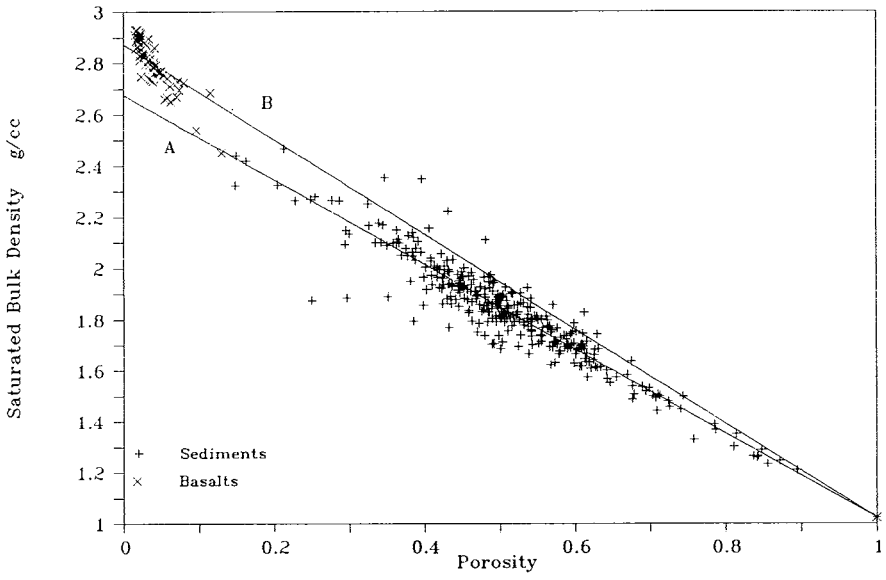

FIGURE 3 Porosity - bulk density plots.

A similar regression through the basalts gives an equivalent grain density of 2.876 ± 0.008 g/cm³, a pore fluid density of 0.967 g/cm³ (slope = -1.909 ± 0.063) with an R^2 of 93.9%. All of these data are well within the expected ranges. The two lines drawn through the data on Figure 3 are based upon a pore fluid density of 1.0245 g/cm³ and grain densities of 2.872 g/cm³ and 2.677 g/cm³ for the upper and lower lines respectively.

POROSITY - VELOCITY TRANSFORMS

Background

Ever since Wyllie et al (1956), the now famous Wyllie time average equation has been universally applied to predict porosities from compressional wave velocities, or visa-versa. The application of the equation has ranged from its routine use in the petrophysical analysis of geophysical borehole logs (Schlumberger, 1972; Dresser Atlas, 1982; Hearst and Nelson, 1985); to lithology and porosity determinations (Domenico, 1984); and algorithms for calculating depth-porosity relationships and understanding subsidence history (Stam et al, 1987).

In their paper Wyllie et al (1956) presented the time average equation, which can be rewritten more conveniently as;

$$\frac{1}{v} = \phi\left(\frac{1}{v_p} - \frac{1}{v_g}\right) + \frac{1}{v_g} \qquad (2)$$

where v is the measured compressional wave velocity of the sample, v_p is the pore fluid velocity and v_g is the matrix velocity of the solid material. This equation, which is often presented in a modified form using travel times rather than velocities, represents a linear relationship between inverse velocity and porosity where the intercept, at ϕ equals zero, is the inverse of the matrix velocity and where the pore fluid velocity can be determined from the slope. The equation was empirically derived from observations on synthetic aggregates of rigid media and produced a satisfactory fit to their data. A less satisfactory fit was observed when applied to rock materials (Wyllie et al, 1958), especially in the high porosity region. The poor fit to this, and other models discussed below, has been attributed to many factors in the subsequent literature including; increased sediment frame bulk modulus and dynamic rigidity caused by overburden pressure, temperature and hydrostatic pressure effects (Fulthorpe and Schlanger, 1989; Gardner et al, 1974)

A plot of inverse velocity against porosity using the ODP Leg 123 data is shown in Figure 4. Linear regression lines are drawn through each of the sediment and basalt data sets (lines A and B

respectively) with no preconceived assumptions other than to include the water point (velocity = 1560 m/s in accordance with the equipment calibration).

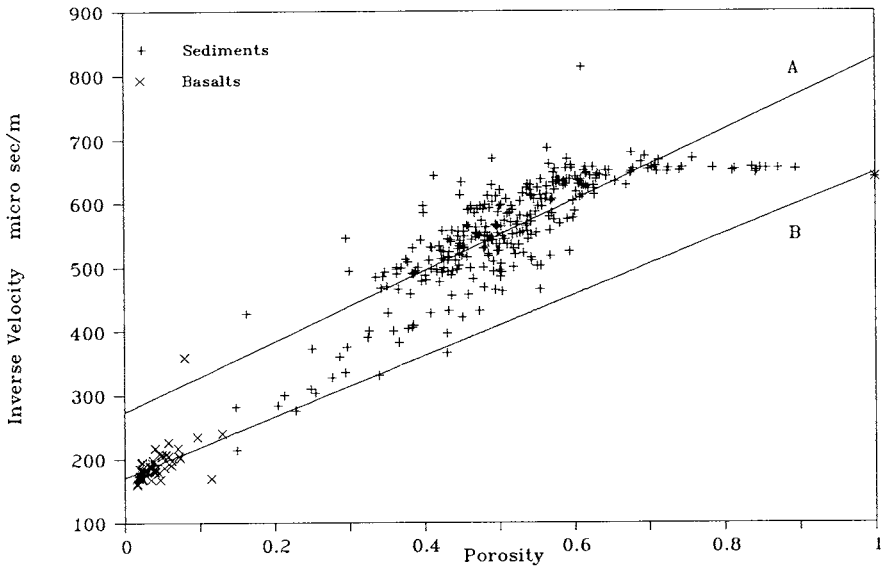

FIGURE 4 Wyllie time average equation plots.

Over the full porosity range the linearity of the data trend is not very convincing but within the range from 30 to 65% a satisfactory line could be drawn. Many porosity-velocity transform practicioners deal with somewhat amorphous clouds of data within this relatively narrow range, which probably explains why the Wyllie time average equation has been adhered to for so long. The levelling off of velocity above 65% porosity corresponds to uncompacted calcareous ooze.

A plot of velocity against porosity is shown in Figure 5 upon which is superimposed plots of velocity derived from equation 2. For line A a v_g value of

6500 m/s for sediments was chosen as being intermediate between the quartz value of 6060 m/s and the calcite value of 6650 m/s (Yale, 1985).

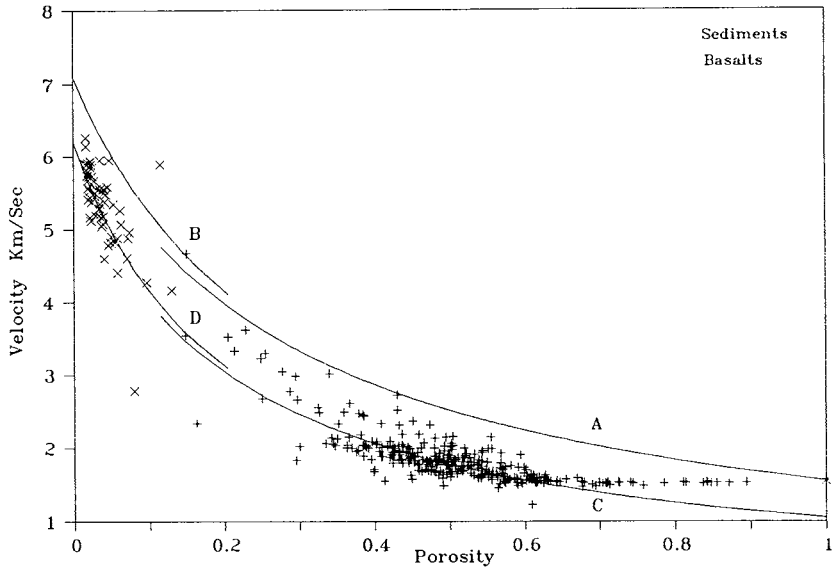

FIGURE 5 Wyllie equation predictions.

A v_g value for basalts (line B) of 7100 m/s was taken as being representative and in both cases a v_p value of 1560 m/s was used, as described above. It can be seen that these two lines do not pass through the data at all and that to force them to do so (lines C and D) requires the somewhat unrealistically low values of 5800, 6200 and 1050 m/s for the sediment and basalt matrix velocities and pore water velocity respectively.

It has long been recognized that the Wyllie equation does not adequately describe the actual relationship between velocity and porosity and there have been many attempts to circumvent these shortcomings. Yale (1985), in a comprehensive review of the literature,

reported wide discrepancies between predicted and measured values of porosity. Han et al (1986) noted that the time average equation significantly overestimates velocities and found it necessary to use unrealistically low values of matrix velocity to accommodate a fit to the data.

Wilkens et al (1986) have used aspect ratio modelling to describe the effect of varying clay content on the porosity-velocity relationship; Castagna et al (1985), Han et al (1986), Taylor-Smith (1974), Anderson (1974) fitted least-squares empirical equations to their data to derive linear relationships between velocity, porosity and clay content; and Rafavich el at (1984) developed linear relationships involving a wide range of petrographic characteristics. The drawback to this sort of approach is that the coefficients derived to fit the empirical equations are specific to the rock materials for which they were determined, thereby limiting their applicability to particular formations and environments. Also there is often no physical basis to justify such equations.

An equally unsatisfactory approach, which is also of limited applicability, has been to modify the time average equation by applying a "compaction correction factor" to account for unconsolidated high porosity materials (Collins and Pilles, 1979; Schlumberger, 1972; Dresser Atlas, 1982). Anderson (1984) simulated the effect on velocity of oil and gas saturation but stressed that his theoretical model was only applicable under those conditions where the time average equation is satisfied.

Pioneering work in the field of the velocity of sound in porous media was carried out by Wood (1941) who showed that for *a suspension of solid particles in a liquid* the mean bulk compressibility equals the sum of the compressibilities of the individual components. Since compressibility is the reciprocal of bulk modulus K, it follows that;

$$\frac{1}{K} = \frac{\phi}{K_p} + \frac{(1-\phi)}{K_g} \tag{3}$$

Also the fundamental equations governing velocity through a perfectly elastic, homogeneous, isotropic solid are given by;

$$\rho_s v_P^2 = K + \frac{4}{3}\mu$$

$$\rho_s v_S^2 = \mu$$

and

$$\sigma = \frac{(v_P^2/v_S^2 - 2)}{2(v_P^2/v_S^2 - 1)}$$

where μ is the rigidity or shear modulus, v_P is the compressional wave velocity, v_S is the shear wave velocity and σ is Poisson's ratio. In the case of a suspension of solid particles in a liquid, the medium will lack rigidity, μ becomes zero and therefore;

$$\frac{1}{\rho_s v^2} = \frac{\phi}{\rho_p v_p^2} + \frac{(1-\phi)}{\rho_g v_g^2} \tag{4}$$

Equation 4 is known as the Wood emulsion equation and can be written more conveniently as;

$$\frac{1}{\rho_s v^2} = \phi\left(\frac{1}{\rho_p v_p^2} - \frac{1}{\rho_g v_g^2}\right) + \frac{1}{\rho_g v_g^2} \tag{5}$$

Equation 5 represents a linear relationship between $1/\rho_s v^2$ and porosity. A plot using the ODP Leg 123 data is shown in Figure 6 with linear regression lines drawn through each of the sediment (line A) and basalt (line B) data sets under the same assumptions as for Figure 4. The linearity of the data is a considerable improvement over the time average equation but there is a significant S shaped characteristic to the plot.

Hamilton (1971) and the McCanns (1968a and 1968b) have shown that while a suspension of solid particles in a liquid can, to a certain extent, be regarded as a two-phase medium, the Wood equation simply puts a lower limit on the magnitude of velocity (Buchan et al, 1971). This can be readily seen in the literature where the Wood equation has been fitted to data; Shumway (1960), Buchan et al (1971), Taylor-Smith (1974), Jackson et al (1981), and Nobes et al (1986). Indeed, Nobes et al (1986) found it necessary to take an empirically weighted mean of

both the Wood and Wyllie equations to compute a better representation to their data over the full range of porosities of Pacific Ocean floor sediments.

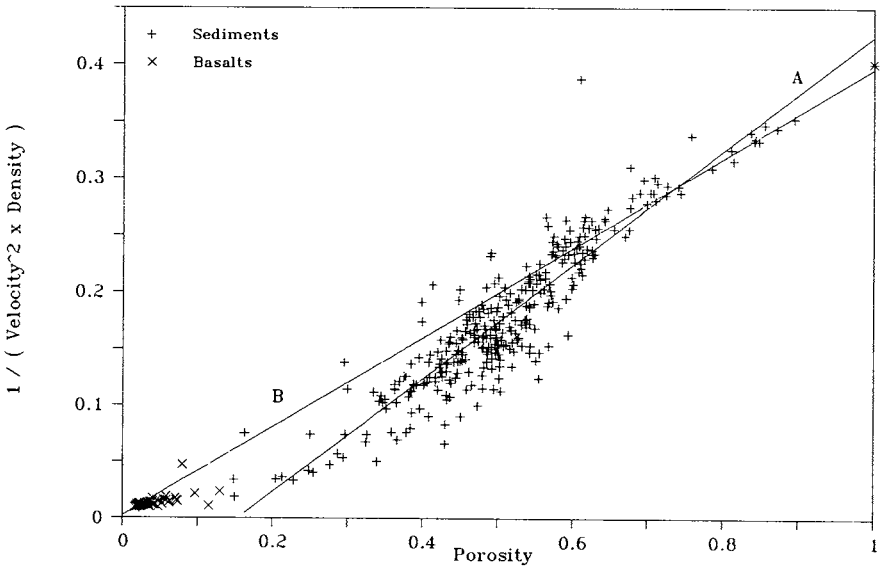

FIGURE 6 Wood emulsion equation plots.

To counteract this minimum limit effect Wyllie et al (1956) introduced the rigidity of the bulk materials and solid matrix into the Wood equation giving the following (presented here in the form of equation 5);

$$\frac{(1+q)}{\rho_s v^2} = \phi\left(\frac{1}{\rho_p v_p^2} - \frac{(1+q_g)}{\rho_g v_g^2}\right) + \frac{(1+q_g)}{\rho_g v_g^2} \qquad (6)$$

where

$$q = \frac{2(1-2\sigma)}{(1+\sigma)} \quad \text{and} \quad q_g = \frac{2(1-2\sigma_g)}{(1+\sigma_g)}$$

Jackson et al (1981) developed a similar argument but presented their equations in the form of compressibilities and the shear wave velocity of the bulk material. Laughton (1957) questioned the validity of equation 3 and argued that when a sediment has been subjected to ever increasing consolidation pressures over geological time, its rigidity increases. He introduced an extra factor to the bulk modulus, K_c, to allow for the resistance to deformation of the structure of the solid particles. Taking this into account the Wood equation becomes (in the form of equation 5);

$$\frac{1}{\rho_s v^2 - K_c} = \phi\left(\frac{1}{\rho_p v_p^2} - \frac{1}{\rho_g v_g^2}\right) + \frac{1}{\rho_g v_g^2} \tag{7}$$

On closer inspection however, because Laughton assumed that structure deformation consists only of shearing strains in the particles and inter-particle bonds, this equation can be seen to be the same as the Wyllie-Wood equation (6) except that the q_g term is missing.

An examination of the Laughton-Wood equation (7) reveals that it has the effect of increasing the entire range of predicted velocity values, including the matrix velocity and the pore water velocity, by an amount equal to $(1+q)^{0.5}$. This is more than 26% for a q value of 0.6 and is clearly not acceptable. The Wyllie-Wood equation has a similar effect at the high porosity end of the range but, if q and q_g are equal, the predicted velocity approaches the matrix velocity at the low end of the range. Clearly, neither Laughton nor Wyllie intended that the inclusion of shear modulus effects in the Wood equation should be applied with equal weight at both the high and low ends of the porosity range. Since the Wood equation was derived to describe loose suspensions of solid particles in a liquid, the inclusion of shear modulus effects should be at a minimum at the higher porosities, increasing

progressively to a maximum at the lower porosities. This can be achieved by multiplying both q and q_g by $(1-\phi)$ so that equation 6 becomes;

$$\frac{(1+q(1-\phi))}{\rho_s v^2} = \phi\left(\frac{1}{\rho_p v_p^2} - \frac{(1+q_g(1-\phi))}{\rho_g v_g^2}\right) + \frac{(1+q_g(1-\phi))}{\rho_g v_g^2} \tag{8}$$

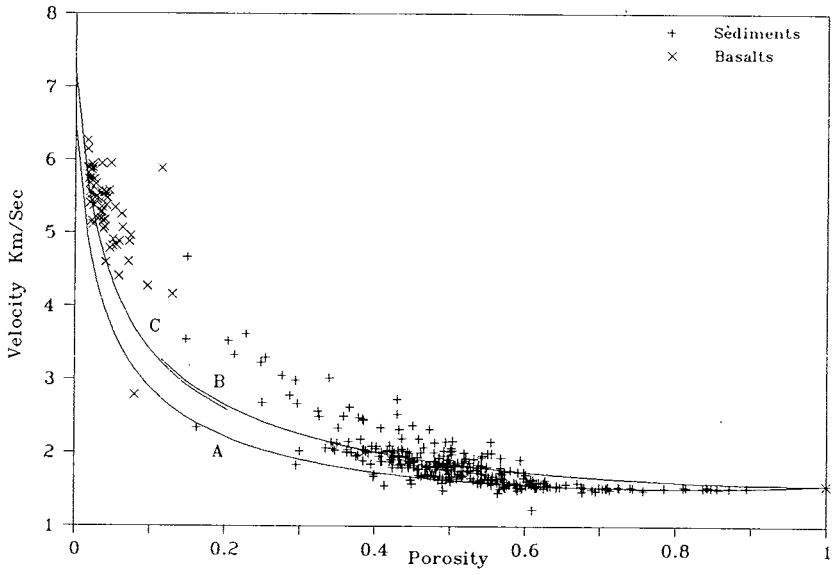

FIGURE 7 Wood emulsion equation predictions.

A plot of velocity against porosity for the ODP Leg 123 data is shown in Figure 7, upon which is superimposed a plot of sediment velocities derived from the Wood equation (line A) using matrix and pore water velocities as before, a pore fluid density of 1.0245 g/cm³, and a grain density of 2.667 g/cm³. The bulk density values were derived from equation 1. Although the overall curvature of this line tends to represent a minimum envelope as described above, it actually plots *through* the data in the porosity range of about 62% to 100%, rather than below it. Therefore, in this porosity range the Wood equation

predicts velocity very well. Also shown in Figure 7 is a plot of velocity predicted from the modified Wyllie-Wood equation (8) for the sediments (line B) and the basalts (line C). These are based upon; sediment parameters as for line A; a basalt matrix velocity of 7100 m/s and grain density of 2.872 g/cm^3; a q_g value of 0.55 derived from a Poisson's ratio of 0.32 (from velocities given in Yale, 1985); and a mean bulk q value of 0.6 derived from a Poisson's ratio of 0.3 (Wyllie et al, 1956; Domenico, 1984). Lines B and C show good correlations between the predicted and measured velocities over most of the porosity range. With unequal values for q and q_g, however, the predicted velocities approach values other than the matrix velocities as the porosity approaches zero. In this case they are 6604 m/s and 7214 m/s for the sediments and basalts respectively.

Nafe and Drake (1957) took a slightly different approach to Wyllie et al (1956) and Laughton (1957) and considered the application of applied pressures to the total system. They made certain empirical assumptions and derived the following equation;

$$v = \phi v_*^2\left(1+\frac{\rho_p}{\rho_s}(1-\phi)\right)+\frac{\rho_g}{\rho_s}v_g^2(1-\phi)^n$$

where v_* is the velocity predicted by the Wood equation (5) and n was suggested to lie between 4 and 5. Nafe and Drake (1957) commented that comparison of their equation with experimental data gave velocities that are too low at the higher porosities and that this could not be improved by different choices of n. This observation is confirmed in Figure 8 where line A is the prediction using the sediment parameters used previously and line B is the prediction using the basalt parameters. In both cases a value for n of 5.5 was needed to reach a moderately acceptable fit to the measured values of velocity from ODP Leg 123 data and even then the predicted values were, in general, too low over the 50 to 100% porosity range and too high over the 0 to 50% range. In order to produce a somewhat more acceptable match, it was necessary to use an unrealistically low matrix velocity of 5800 m/s, as shown in line C (the model is relatively insensitive to grain density variations).

More recently, in the development of porosity-velocity transforms, Raymer el at (1980)

presented three algorithms to describe the upper and lower porosity ranges separately and a linear interpolation to link the two.

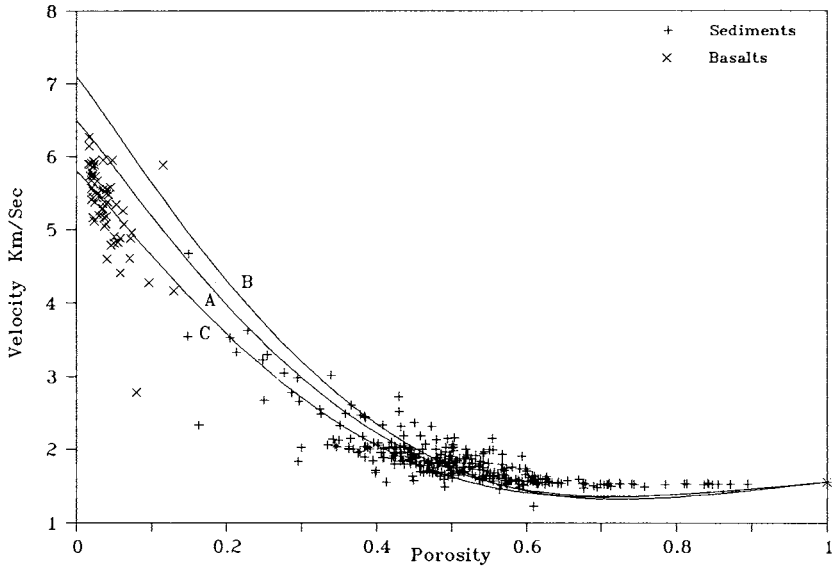

FIGURE 8 Nafe and Drake equation predictions.

The first two algorithms were given as alternatives for the 0 to 37% range and are;

$$v = \left(\frac{\rho_g}{\rho_s}\right)^{0.5} (1-\phi)^{1.9} v_g \tag{9}$$

and

$$v = \phi v_p + (1-\phi)^2 v_g \tag{10}$$

The third Raymer et al (1980) algorithm, to describe the 47 to 100% range, was stated to be totally empirical but is in fact the Wood equation (though not attributed as such). Raiga-Clemenceau et al (1988) introduced the concept of acoustic formation

factor to describe the velocity-porosity relationship in the 0 to 50% porosity range. Their empirically derived equation is of the form;

$$v = v_g(1-\phi)^x \tag{11}$$

where the exponent x was taken to be 1.76 for a calcite matrix.

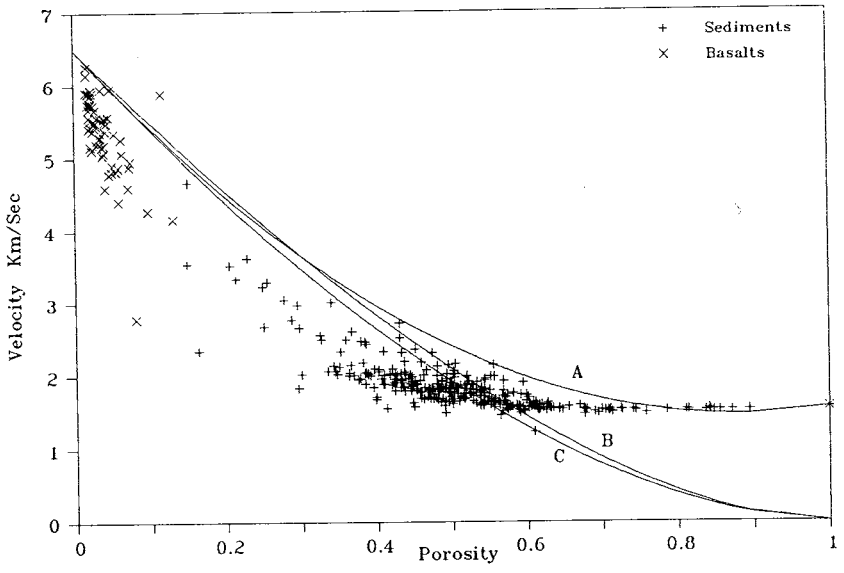

FIGURE 9 Raymer and Raiga - Clemenceau equation predictions.

Velocities derived from equations 9 (line B), 10 (line A) and 11 (line C) are shown in Figure 9 using the sediment parameters only: matrix velocity = 6500 m/s throughout; pore fluid velocity = 1560 m/s for line A; pore fluid density = 1.0245 g/cm^3, grain density = 2.667 g/cm^3 and bulk density values derived from equation 1 for line B; and exponent x = 1.76

for line C. As claimed by Raymer et al (1980), lines A and B are virtually the same over the 0 to 37% porosity range while the Raiga-Clemenceau et al (1988) line C is almost the same as line B over the entire porosity range. The Raiga-Clemenceau et al (1988) algorithm does not, therefore, differ significantly from the Raymer et al (1980) algorithms and they all predict consistently higher velocities than those measured for the ODP Leg 123 samples, in much the same way as the Wyllie time average equation.

The Acoustic Impedance Transform

The well defined data relationship between porosity and velocity spawned much of the work discussed in the previous section. An equally well defined relationship between bulk density and velocity has also long been recognised, and the use of acoustic impedance (the product of velocity and bulk density) to determine reflection coefficients is an established tool in seismic interpretation (Rafavich et al, 1984). Gardner et al (1974) derived an empirical exponential relationship between density and velocity based upon reflection coefficient considerations. The close linearity between porosity and reflection coefficient is relatively well documented (Buchan et al, 1971; Taylor-Smith, 1974) but does not seem to have been explored as the basis of a potential porosity-velocity transform.

Following the lead given by Wood and Wyllie, a plot of inverse acoustic impedance against porosity is shown in Figure 10 using the ODP Leg 123 data, with linear regression lines drawn through each of the sediment (line A) and basalt (line B) data sets under the same assumptions as for Figure 4. The linearity of the data is clear and is significantly better than that for the Wood equation (Figure 6). These linear regression lines are represented by the following equation;

$$\frac{1}{\rho_s v} = \phi\left(\frac{1}{\rho_p v_p} - \frac{1}{\rho_g v_g}\right) + \frac{1}{\rho_g v_g} \qquad (12)$$

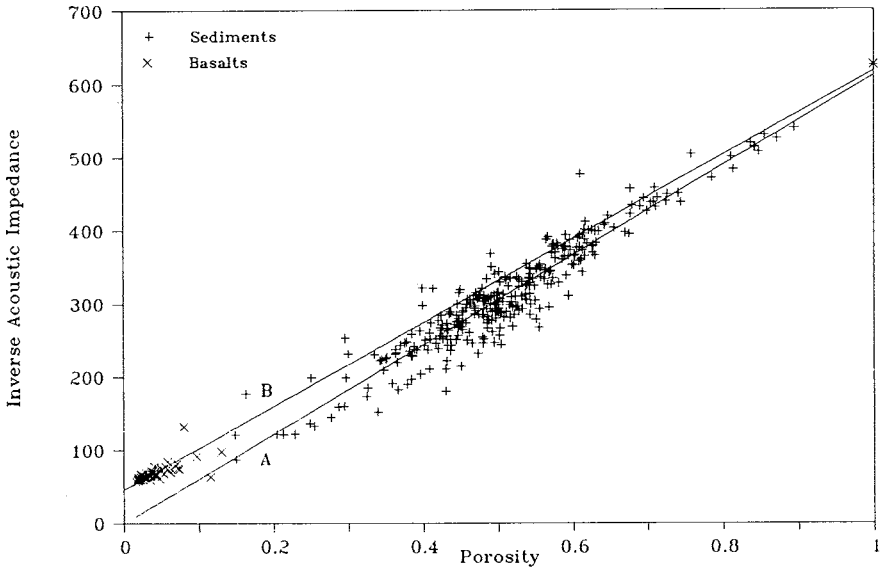

FIGURE 10 Acoustic impedance equation plots.

Figure 11 shows a plot of velocities derived from equation 12 (line A) superimposed upon the Leg 123 velocity-porosity data using the same sediment parameters as before. For direct comparison, the velocities derived from the Wood equation (5), previously shown as Line A, Figure 7, are also shown in Figure 11. It is clear that while the original Wood equation is a better predictor of velocities over the 45 to 100% porosity range, equation 12 predicts the velocities more closely over the 0 to 45% porosity range. Indeed, over the entire porosity range, equation 12 tends to represent a closer approximation to a minimum envelope to the data than has been postulated for the Wood equation.

Using a similar line of argument to that which led to the development of equation 8, equation 12 can be modified in the following way;

$$\frac{(1+q(1-\phi))}{\rho_s v} = \phi\left(\frac{1}{\rho_p v_p} - \frac{(1+q_g(1-\phi))}{\rho_g v_g}\right) + \frac{(1+q_g(1-\phi))}{\rho_g v_g} \qquad (13)$$

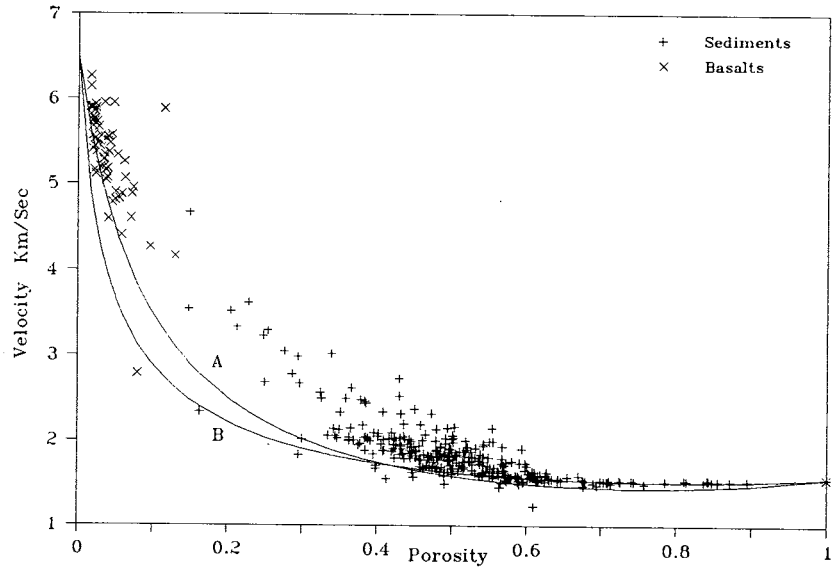

FIGURE 11 Acoustic impedance and Wood equation predictions.

This is a semi-empirical equation based in part upon the fully validated concepts of acoustic impedance. When the velocities predicted by this equation are compared to the ODP Leg 123 data, using the same sediment and basalt parameters as used in Figure 7, (ie; a sediment matrix velocity of 6500 m/s, a sediment grain density of 2.667 g/cm^3, a basalt matrix velocity of 7100 m/s, a basalt grain density of 2.872 g/cm^3, a pore water velocity of 1560 m/s, a pore fluid density of 1.0245 g/cm^3, and bulk density values derived from equation 1) they tend to be a little too high over the higher porosity range. However, adjusting q and q_g to be both equal to 0.22 (equivalent to a Poisson's ratio of 0.42) results in lines A and B shown in Figure 12 for the sediments and basalts respectively.

The velocity values predicted by the acoustic impedance equation above, achieve a very much closer fit to the measured values of velocity than those predicted by the modified Wyllie-Wood equation over

both the upper and lower porosity ranges. The adjustment to the q values in the acoustic impedance equation is considered acceptable because of the semi-empirical nature of equation 13, but a Poisson's ratio of 0.42 is still within the range of values presented in the literature for limestones and sandstones.

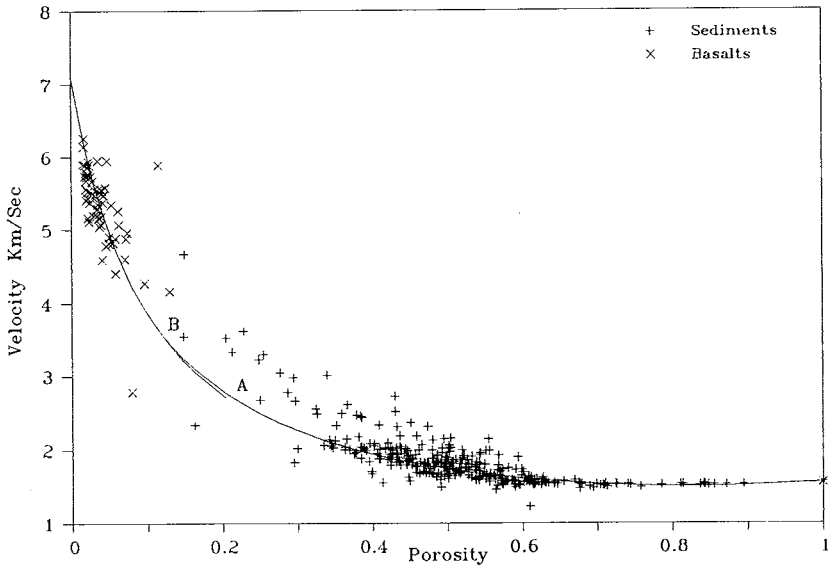

FIGURE 12 Modified acoustic impedance equation predictions.

A similar adjustment to the q values used in the modified Wyllie-Wood equation may be less acceptable, because of the firm basis of this equation in elasticity theory, but if the q values used in equation 8 are both reduced to 0.45 (equivalent to a Poisson's ratio of 0.35) then a better fit to the data can be achieved. Even so this fit is still not as close as that represented by lines A and B in Figure 12.

A more accurate representation of predicted

velocities for individual samples will, of course, be obtained by using the measured values of grain density and bulk density rather than derived values of bulk density from equation 1 and average grain densities. This procedure does not, however, give smooth curves for the purposes of comparing the velocity predictions of one model against another. As a measure of the correlation between the predicted and measured values of velocity the values derived from equations 8 and 13 were re-calculated using the measured grain and bulk densities for each sample. A linear regression equation was then calculated for the predicted velocities, derived from each of the acoustic impedance and the modified Wyllie-Wood equations, against the measured values of velocity. A perfect correlation would result in a slope of 1, an intercept of 0 and an R^2 of 100. The values for the acoustic impedance equation were 0.90 ± 0.01, 144 ± 250 and 96 respectively and those for the modified Wyllie-Wood equation were 0.70 ± 0.01, 455 ± 245 and 95.

DISCUSSION AND CONCLUSIONS

The limitations of the Wyllie time average equation have been know for many years and have been re-emphasised here by comparing predicted and measured compressional wave velocities of marine samples ranging from oozes, close to the sea-sediment interface, through to basement basalts.

Some of the limitations of the time average equation were also recognised by Wyllie and his co-workers who amended the Wood emulsion equation to partially take account of the rigidity of the materials. Further modifications to this Wyllie-Wood equation have been shown here to not only describe the relationship between porosity and velocity more closely than the time average equation, but also more closely than some of the alternatives proposed by contemporaries of Wyllie and since. Indeed, bearing in mind the Wyllie-Wood equation was discussed in the same paper the time average equation was first proposed, it is somewhat curious that the time average equation has been adhered to for so long. Furthermore, it is curious that some of the more recent publications do not seem to take account of, or even be aware of, the pioneering research carried out in this field in the 1950's.

A semi-empirical acoustic impedance relationship has been developed which is shown to provide a more accurate porosity-velocity transform, using realistic material parameters, than has hitherto been possible. The fact that a closer correlation can be achieved with this semi-empirical equation, than with the more theoretically based modified Wyllie-Wood equation, perhaps opens to question some of the fundamental assumptions governing compressibilities of materials upon which this early work was based.

If enough is known about the lithology to provide estimates of the matrix and pore water parameters, equations 13 and 1 enable a complete description of the behaviour of a saturated rock core in terms of compressional wave velocity, porosity and bulk density. If measurements of bulk density and grain density are also available then it allows average values of some of these parameters to be determined or alternatively removes the necessity of assuming grain densities for each sample.

ACKNOWLEDGEMENTS

Robin Brereton wishes to thank Michael Riggins, fellow Physical Properties Specialist during Leg 123; John Ludden and Felix Gradstein, the two Co-Chief Scientists; Andrew Adamson, the ODP Staff Scientist; and all the scientific party and crew of JOIDES Resolution during the cruise. This paper is published with permission of the Director, British Geological Survey (NERC).

REFERENCES

ANDERSON, R. A., 1984. Fluid and frequency effects on sonic velocities. SPWLA Trans., 25_{th} Logging Symposium, Paper AAA.

ANDERSON, R. S., 1974. Statistical correlation of physical properties and sound velocity in sediments. In: Hampton, L., Ed. Physics of Sound in Marine Sediments. Plenum Press, New York and London.

BRERETON, N. R., 1990. Physical properties of sediments and basalts from the Argo and Gascoyne Abyssal Plains in the Indian Ocean. British Geological Survey Technical Report. WK/90/11.

BOYCE, R. E., 1976. Definition and laboratory

techniques of compressional sound velocity parameters and wet-water content, wet-bulk density, and porosity parameters by gravimetric and gamma ray attenuation techniques. In Shlanger, S.O., Jackson, E.D., et.al., Init. Repts. DSDP, 33: Washington (U.S. Govt. Printing Office), 931-958.

BUCHAN, S., DEWES, F. C. D., JONES, A. S. G., MCCANN, D. M., and TAYLOR-SMITH, D., 1971. The acoustic and geotechnical properties of North Atlantic cores. University College of North Wales, Marine Science Laboratories, Geological Report 71-1.

CASTAGNA, J. P., BATZLE, M. L. and EASTWOOD, R. L., 1985. Relationships between compressional-wave and shear-wave velocities in clastic silicate rocks. Geophysics, **50** (4), 571-581.

COLLINS, H. N., and PILLES, D., 1979. Some uses of functional analysis in petrophysics. 7th Formation Evaluation Symposium of the Canadian Well Logging Society.

DOMENICO, S. N., 1984. Rock lithology and porosity determinations from shear and compressional wave velocity. Geophysics, **49** (8), 1188-1195.

DRESSER ATLAS. 1982. Well logging and interpretation techniques.

FULTHORPE, C. S., and SCHLANGER, S. O., 1989. In situ acoustic properties of pelagic carbonate sediments on the Ontong Java Plateau. J. Geophys. Res., **94**, 4025-4032.

GARDNER, G. H. F., GARDNER, L. W., and GREGORY, A. R., 1974. Formation velocity and density - the diagnostic basics for stratigraphic traps. Geophysics, **39** (6), 770-780.

HAMILTON, E. L., 1971. Elastic properties of marine sediments. J. Geophys. Res., **76** (2), 579-604.

HAMILTON, E. L., 1974. Prediction of deep-sea sediment properties: state-of-the-art. In: Inderbitzen, A. L., Ed. Deep-sea sediments. Plenum Press, New York and London.

HAN, D., NUR, A., and MORGAN, D., 1986. Effects of porosity and clay content on wave velocities in sandstone. Geophysics, **51** (11), 2093-2107.

HEARST, J. R., and NELSON, P. H., 1985. Well logging for physical properties. McGraw-Hill.

JACKSON, P. D., BARIA, R., and McCANN, D. M., 1981. Geotechnical assessment of superficial marine sediments using in-situ geophysical probes. Ocean Management, **7**, 189-209.

LAUGHTON, A. S., 1957. Sound propagation in compacted ocean sediments. Geophysics, **22** (2),

233-260.

McCANN, C., 1968a. An investigation of the acoustic properties of natural materials. Unpubl. PhD Thesis, University of Wales, Bangor.

McCANN, D. M., 1968b. The acoustic properties of North Atlantic cores. Unpubl. PhD Thesis, University of Wales, Bangor.

NAFE, J. E., and DRAKE, C. L., 1957. Variation with depth in shallow and deep water marine sediments of porosity, density and the velocities of compressional and shear waves. Geophysics, **22** (3), 523-552.

NOBES, D. C., VILLINGER, H., DAVIS, E. E., and LAW, L. K., 1986. Estimation of marine sediment bulk physical properties at depth from seafloor geophysical measurements. J. Geophys. Res., **91**, 14033-14043.

ODP LEG 123 SHIPBOARD SCIENTIFIC PARTY. 1989a. Ocean Drilling Program - the birth of the Indian Ocean. Nature, **337** (9 February), 506-507.

ODP LEG 123 SHIPBOARD SCIENTIFIC PARTY. 1989b. ODP investigates Indian Ocean origins. Geotimes **34** (3), 16-19.

ODP LEG 123 SHIPBOARD SCIENTIFIC PARTY. 1990. Proceedings of the Ocean Drilling Program - Initial Reports. Vol 123 - Argo Abyssal Plain and the Gascoyne Abyssal Plain. Sites 765-766, September - November, 1988. National Science Foundation. Joint Oceanographic Institutions, Inc. [*in press*].

RAFAVICH, F., KENDALL, C. H. ST. C., and TODD, T. P., 1984. The relationship between acoustic properties and the petrographic character of carbonate rocks. Geophysics, **49** (10), 1622-1636.

RAIGA-CLEMENCEAU, J., MARTIN, J. P., and NICOLETIS, S., 1988. The concept of acoustic formation factor for more accurate porosity determination from sonic transit time data. The Log Analyst, Jan-Feb, 1988.

RAYMER, L. L., HUNT, E. R., and GARDNER, J. S., 1980. An improved sonic transit time-to-porosity transform. SPWLA Trans., 21_{st} Logging Symposium, Paper P.

SCHLUMBERGER. 1972. Log interpretation principles.

SHUMWAY, G., 1960. Sound and absorption studies of marine sediments by a resonance method, parts I and II. Geophysics, **25**, (2) 451-467, and (3) 659-682.

STAM, B., GRADSTEIN, F. M., LLOYD, P., and GILLIS, D., 1987. Algorithms for porosity and subsidence history. Computers and Geosciences, **13** (4), 317-349.

TAYLOR-SMITH, D., 1974. Acoustic and mechanical

loading of marine sediments. In: Hampton. L., Ed. Physics of sound in marine sediments. Plenum Press, New York and London.

WILKENS, R. H., SIMMONS, G., WISSLER, T. M. and CARUSO, L., 1986. The physical properties of a set of sandstones - part III. The effects of fine-grained pore filling material on compressional wave velocity. Int. J. Rock Mech. Min. Sci. & Geomech. Abstr. **23** (4), 313-325.

WOOD, A. B., 1941. A textbook of sound. The Macmillan Company, New York.

WYLLIE, M. R. J., GREGORY, A. R., and GARDNER, L. W., 1956. Elastic wave velocities in heterogeneous and porous media. Geophysics, **21** (1), 41-70.

WYLLIE, M. R. J., GREGORY, A. R., and GARDNER, G. H. F., 1958. An experimental investigation of factors affecting elastic wave velocities in porous media. Geophysics, **23** (3), 459-493.

YALE, D. P., 1985. Recent advances in rock physics. Geophysics, **50** (12), 2480-2491.

IMAGING